

ACTIVE 2006

18-20 SEPTEMBER 2006

ADELAIDE AUSTRALIA

Nonlinear models of electro pneumatic transducers for use in feedforward active noise control schemes

André Jakob^a, Michael Möser

Institut für Technische Akustik, Technische Universität Berlin
Einsteinufer 25, Sekr. TA7, 10587 Berlin
Germany

ABSTRACT

In order to yield high sound amplitudes at low frequencies in active noise control applications a electro pneumatic transducers as alternatives to commonly used electro dynamic loudspeakers are suggested in literature. Such a sound source consisting of a modulated air flow was investigated and control algorithms for this kind of nonlinear secondary sources were developed. Two models of this nonlinear secondary path were investigated: firstly, a black box model consisting of a time delay neural network (TDNN) and, secondly, a white box, respectively grey box, model derived directly from the underlying differential equations and a time discrete version of it, with partly estimated parameters. The details of modelling of the analytical model is shown and some general remarks on the modelling of the TDNN secondary path model are given.

1 INTRODUCTION

The aim of this paper is to find models of an electro pneumatic transducer² suitably to fit into the feedforward active noise control scheme. This means that a time-discrete input-output model, from which the output of the secondary source can directly be calculated in every time step by current and past input signal values and current and past output or internal signal values. Nevertheless, once the nonlinear models are built they cannot simply be inserted into the filtered-x LMS algorithm used with linear models, e.g. FIR filter models. Instead new algorithms must be developed, which consider the nonlinear behavior of the nonlinear secondary path models.

In [1] an algorithm is derived which can be used with neural network secondary path models and neural network controllers for feedforward control. In [2] a simplification of this algorithm is given for the control of harmonic sound which uses a simple FIR filter as controller in conjunction with the neural network secondary path model instead of the neural network controller. This greatly reduces the computational effort necessary for adaptation and execution of the controller. In both cases it turns out, that in contrast to the filtered-x LMS algorithm the adaptation algorithm with nonlinear secondary paths not only needs the output signal of the secondary path model but the internal states of the secondary path model too. In [3] is shown that the FIR filter controller performs equally well or even better than the neural network controller with harmonic sound provided that care has to be taken regarding the correct size of the controller.

Electro pneumatic sound sources modulate an air-flow through small orifices in order to generate tones corresponding to the frequency of the modulation. Unfortunately, in practical setups some nonlinearities occur, so that higher harmonics are excited along with the fundamental frequency. The nonlinearities are discussed in the next section.

^aEmail address: andre.jakob@tu-berlin.de

²Sometimes called electro pneumatic sound source or compressed-air loudspeaker

In the past electro pneumatic sound sources were investigated by Chapman and Glendinning [4] and by Glendinning, Nelson and Elliott [5]. The sound source was called a sonic source because the flow velocity of the air through the orifices was higher than the speed of sound. Blondel and Elliott [6] investigated a sub-sonic source and stated, that the efficiency of the sub-sonic source is higher than that of the sonic source.

2 ANALYTICAL SECONDARY PATH MODEL

Figure 1 shows a sketch of an electro pneumatic sound source. It is a similar setup as in [5, 6]. A slider with orifices (holes or slits) is moved back and forth in one direction against a stator with the same orifices. Slider and stator are the output of a plenum chamber, which is supplied with compressed air. The slider is moved by means of a

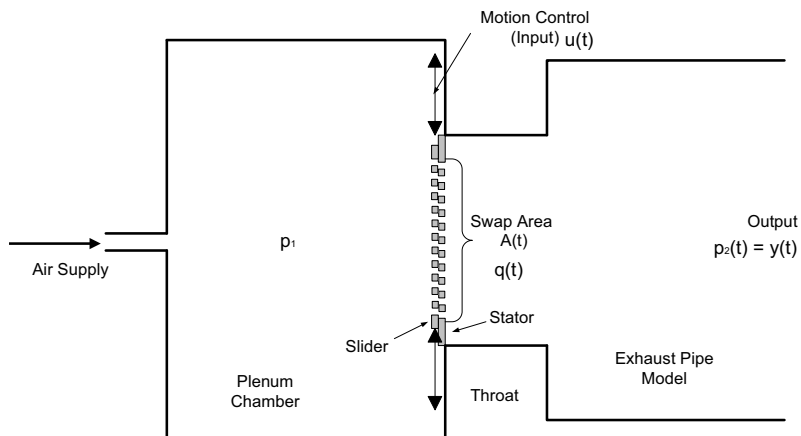


Figure 1: Sketch of the electro pneumatic transducer

and thus the movement of the slider are in the order of less than 1 mm. The construction of the analytical model is performed in two steps, here, i.e. firstly, construction of a time-continuous model with the underlying differential equations and, secondly, translation of the time-continuous model into a time-discrete model.

2.1 Time-continuous model

A shaker behaves like a loudspeaker, thus the governing equations are similar. On the electrical side the electrical current $I(t)$ through the voice coil is related to its input voltage $U_e(t)$ and the resulting velocity $v(t)$ of the voice coil via

$$U_e(t) = RI(t) + L\dot{I}(t) + Blv(t), \quad (1)$$

wherein R is the electrical resistance of the voice coil, L is its inductance, $\dot{I}(t)$ denotes the time derivative of the current and Bl is the magnetic field strength times the length of the coil (cf. eg. [7]). Bl is often called the transfer factor. On the mechanical side the driving force $BII(t)$ equals the force due to the inertia of the mass, i.e. $ma(t)$ with $a(t)$ being the acceleration of the voice coil, the friction force due to the friction between slider and stator and the force $sx(t)$ due to the centering spring of the shaker with $x(t)$ being the displacement of the voice coil. Thus,

$$BII(t) = ma(t) + F_R \{v(t)\} + sx(t). \quad (2)$$

The friction is a nonlinear function of the slider's velocity. Here the friction curve (without hysteresis) is assumed to be

$$F_R \{v(t)\} = \text{sign}(v(t)) \cdot [(\mu_h - \mu_g) \cdot e^{-\alpha_1|v(t)|} - \mu_h \cdot e^{-\alpha_2|v(t)|} + \mu_g] , \quad (3)$$

wherein μ_h and μ_g are static and dynamic friction coefficients respectively. α_1 and α_2 influence the slopes of the curve. The resulting area of the orifices is a function of the displacement of the shaker, which can be nonlinear, too, i.e.

$$A(t) = F_A \{x(t)\} . \quad (4)$$

$F_A \{x(t)\}$ is a nonlinear function if the orifices are fully aligned for zero voltage at the input of the shaker, i.e. an absolute value function is included, because $A(t)$ becomes smaller in both directions of the slider movement. For circular orifices another weak non-linearity exists due to the shape of the holes, which is not present for rectangular orifices. Of course, when the displacement of the slider movements exceeds the diameter of the orifices clipping occurs, which is another strong nonlinearity.

The pressure difference Δp is assumed here to be constant and is related to the flow velocity $u(t)$ (averaged over the diameter of the tube) via

$$\Delta p = C_D(t) \frac{1}{2} \rho u(t)^2 \quad \leadsto \quad u(t) = \sqrt{\frac{2\Delta p}{C_D(t)\rho}} =: F_u \{C_D(t)\} , \quad (5)$$

ρ being the density of air. Δp is the difference of the static pressure on both sides of the slider. The plenum is assumed to be large enough to avoid fluctuations of the static pressure inside it. Note, that the discharge coefficient $C_D(t)$ is assumed here to be time dependent, thus the same applies to the flow velocity $u(t)$. The discharge coefficient depends on the shape of the orifices not on their size. When circular orifices are considered, the shape varies from fully circular to narrow lenticular in each cycle of the moving slider. Thus, $C_D(t)$ depends on $x(t)$, i.e.

$$C_D(t) = F_{CD} \{x(t)\} . \quad (6)$$

A procedure for determining F_{CD} can be as follows: measure the flow velocity for different fixed positions x of the slider together with the static pressure difference Δp , calculate the different discharge coefficients according to Equation 5 and find some function that approximates the measured values.

The volume flow $q(t)$ is the change of volume $V(t)$ with time t and is related via the flow velocity $u(t)$ and the orifice area $A(t)$ via

$$q(t) = \frac{\partial V(t)}{\partial t} = u(t) \cdot A(t) . \quad (7)$$

The resulting time-continuous block diagram is shown in Figure 2.

The sound pressure at the error microphone inside the exhaust tube can be obtained as follows: For convenience the sound pressure in tube regions ① and ② respectively will be calculated in frequency domain here. It can be formulated as follows (cf. Figure 3 (left)):

$$p_1(x) = A \cdot [e^{+jk(x+l_1)} + r_1 e^{-jk(x+l_1)}] , \quad (8)$$

$$p_2(x) = B \cdot [e^{-jk(x-l_2)} + r_2 e^{+jk(x-l_2)}] . \quad (9)$$

From Figure 4 the difference equations for the slider displacement, slider velocity and voice coil current can easily be read, i.e.

$$x(n) = x(n-1) + \frac{T}{2} [v(n) + v(n-1)], \quad (18)$$

$$v(n) = v(n-1) + \frac{T}{m} [BlI(n-1) - F_R \{v(n-1)\} - sx(n-1)], \quad (19)$$

$$I(n) = I(n-1) + \frac{T}{2L} [U_e(n) - Blv(n) - RI(n) + U_e(n-1) - Blv(n-1) - RI(n-1)]. \quad (20)$$

Time-discrete slider opening area $A(n)$, volume flow $q(n)$, discharge coefficient $C_D(n)$ and flow velocity $u(n)$ are given by

$$A(n) = F_A \{x(n)\}, \quad q(n) = u(n) \cdot A(n), \quad (21)$$

$$C_D(n) = F_{CD} \{x(n)\}, \quad u(n) = F_u \{C_D(n)\}. \quad (22)$$

The resulting time-discrete sound pressure inside region ② of the attached tube is obtained as follows: Firstly, measure the complex reflection coefficients $r_1(\omega)$ and $r_2(\omega)$. Secondly, calculate the complex frequency response of the sound pressure $p_2(\omega)$ at a given position x by means of Equation 9 and Equation 15. Thirdly, design a FIR-Filter with the calculated frequency response. The input of the filter is $q(n)$ and its output equals $p_2(n)$ at position x , where the error microphone is located. It should be noted, that the filter also should include the delay due to the analogue-to-digital and digital-to-analogue conversion, which is not included in Figure 4.

2.3 Identification of the time-discrete model

Some parameters of the system can easily be measured directly or are given in the manual of the shaker, e.g. the electrical resistance R of the shaker or the mass m of slider and voice coil. Of course, the parameter T , i.e. the sampling time, is given per definition. Other parameters cannot be measured directly particularly the parameters μ_h , μ_g , α_1 and α_2 of the friction curve, Equation 3. Other parameters not directly available are the transfer factor Bl and the discharge coefficients C_D . The discharge coefficients C_D , i.e. the function $F_{CD} \{x(t)\}$, can be measured with the method pointed out in section 2.1.

It might be helpful to identify parts of the system. E.g. while the transfer factor Bl , stiffness s of the voice coil spring and inductance L are examined, it is useful to separate shaker and slider from the sound source and measure the acceleration response due to some random input voltage. Identifying these parameters with dismantled shaker and slider is easier, because the system behaves linear in this arrangement. An example of the identification of some parameters is given below.

After identifying the (linear) parameters of the shaker the other parameters, i.e. the friction curve, can be identified with shaker and slider mounted inside the sound source. The friction depends on the pressure inside the plenum because this yields in a force acting on the slider and pressing it against the stator. Increasing the plenum pressure thus increases friction between slider and stator.

The two other functions $F_A \{x(t)\}$ and $F_u \{C_D(t)\}$ are given a priori, the first by pure geometric considerations and the latter by Equation 5.

In the mechanical part a priori unknown parameters are the transfer factor Bl and the parameters μ_h, μ_g, α_1 and α_2 of the friction curve. Here a simple method to adapt the parameters with a 'LMS-type' algorithm and simulation results obtained with it are given. A 'LMS-type' algorithm for the adaptation of Bl is

$$Bl(n+1) = Bl(n) - \nu \nabla_e(n), \quad (23)$$

wherein ν is a step size parameter and $\nabla_e(n)$ is the gradient of some error function with respect to $Bl(n)$. Here the acceleration of the slider is used for the generation of the error signal $e(n) = \hat{a}(n) - a(n)$, with $\hat{a}(n)$ being the measured acceleration and $a(n)$ being the acceleration inside the model. The gradient then becomes

$$\nabla_e(n) = \frac{\partial e(n)^2}{\partial Bl(n)} = 2e(n) \frac{\partial e(n)}{\partial Bl(n)} = -2e(n) \frac{\partial a(n)}{\partial Bl(n)}. \quad (24)$$

When reading from the block diagram in Figure 4, that

$$a(n) = \frac{1}{m} [BlI(n) - F_R\{v(n)\} - sx(n)] \quad (25)$$

one directly obtains a simple rule for the adaptation of Bl

$$Bl(n+1) = Bl(n) + 2\nu e(n) \frac{1}{m} I(n). \quad (26)$$

Similarly can be derived adaptation rules for the parameters of the friction curve (cf. Equation 3) by evaluating the derivatives of Equation 25 with respect to each individual friction parameter. This yields

$$\mu_h(n+1) = \mu_h(n) + 2\nu e(n) \frac{1}{m} \cdot \text{sign}(v(n)) \cdot [e^{-\alpha_1|v(n)|} - e^{-\alpha_2|v(n)|}], \quad (27)$$

$$\mu_g(n+1) = \mu_g(n) + 2\nu e(n) \frac{1}{m} \cdot \text{sign}(v(n)) \cdot [-e^{-\alpha_1|v(n)|} + 1], \quad (28)$$

$$\alpha_1(n+1) = \alpha_1(n) - 2\nu e(n) \frac{1}{m} \cdot v(n) \cdot (\mu_h - \mu_g) \cdot e^{-\alpha_1|v(n)|}, \quad (29)$$

$$\alpha_2(n+1) = \alpha_2(n) + 2\nu e(n) \frac{1}{m} \cdot v(n) \cdot \mu_h \cdot e^{-\alpha_2|v(n)|}. \quad (30)$$

Figure 5 to Figure 7 show simulation results. A fixed model is used in the simulation as the 'true' system. Its parameters were chosen according to physical insight and to some trial and error procedure with measured signals. The parameters were $T = 1$ ms, $L = 0.27$ mH, $R = 1.9 \Omega$, $Bl = 2$ Tm, $m = 55$ g, $s = 3500$ N/m, $\mu_h = 1.2$, $\mu_g = 1.0$, $\alpha_1 = 1$, $\alpha_2 = 20$.

In Figure 5 are shown results of the adaptation of Bl in the model, which is assumed to be unknown, for random noise excitation. In Figure 5a) all other parameters are assumed to be known exactly. It can be seen, that Bl converges to the value of the 'true' system. The error signal $e(n)$ behaves not as it would behave, when the system would be purely linear. It shows a lot of 'spikes' while the adaptation process which disappear when the

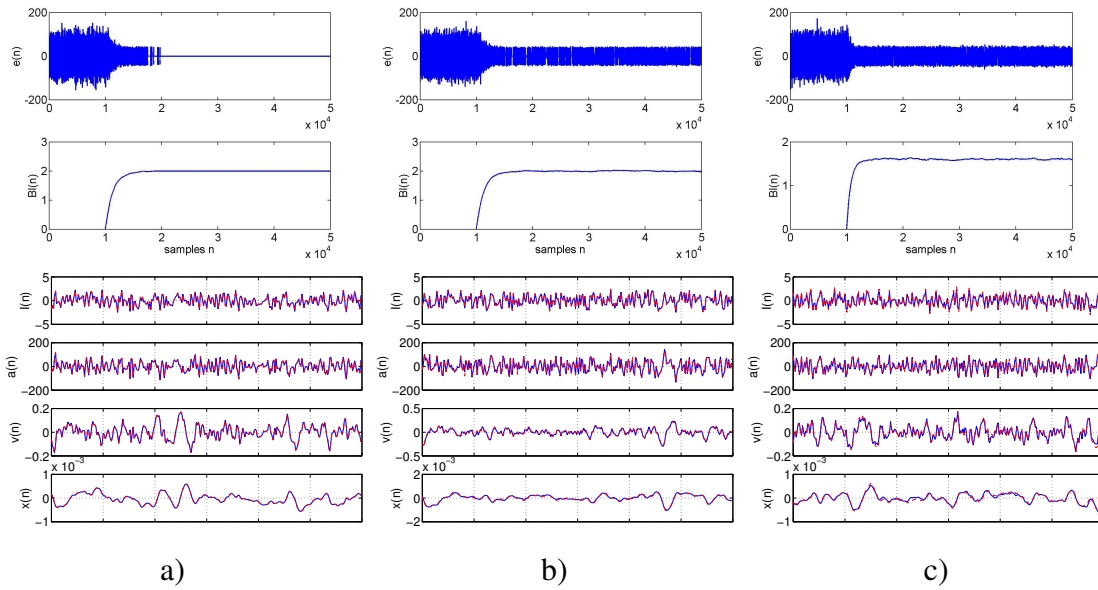


Figure 5: Simulation results, adaptation of Bl , a): all other model parameters exactly initialized, b): model friction parameters $\alpha_1 = 2$ and $\alpha_2 = 15$, c): resistance in the model $R = 1.5\Omega$. Displayed are $e(n)$ and $Bl(n)$ over the whole simulation period and short intervals of $I(n)$, $a(n)$, $v(n)$ and $x(n)$ at the end of the simulation.

adaptation is sufficiently good. This can be explained by the nonlinearity in the system and the chosen error signal: When the acceleration signal $a(n)$ is investigated with a pure sinusoidal input (cf. e.g. Figure 6) it shows very steep rising and falling edges. When the acceleration signals of the 'true' system and the estimated model differ slightly in phase the error signal gets a spike at these steep edges.

Figure 5b) shows results of the Bl -adaptation for a non-perfectly estimated friction curve in the model. In the case shown Bl still converges to the desired value in the mean. The error signal pretends a bad adaptation, whereas a look upon the signals of the 'true' system (blue lines) and estimated model (red dashed lines) shows a very good match. However, if only a very bad estimate of the friction curve would be available, the adaptation of Bl could be done without the nonlinear part as indicated at the beginning of this section.

To some extend the adaptation of Bl can overcome problems with bad measurements or estimations of other parameters. Figure 5c) shows a result with $R = 1.5\Omega$ in the model (keeping $R = 1.9\Omega$ in the 'true' system). In that case Bl simply converges to another value (1.6 Tm) and again the error looks bad but the signals match very good.

Figure 6 and Figure 7 show the effect of adapting the friction curve according to Equations 27 to 30. This is done with a sinusoidal signal rather than a random signal, because it was observed that the algorithm is more stable with it and the dynamics of the system are determined mainly by the other parameters already estimated. At least the parameters α_1 and α_2 of the friction curve must be initialized with values different from zero, as can be seen from their adaptation rules. For a reasonable initial guess of the parameters physical insight about the generic shape of the friction curve can be used,

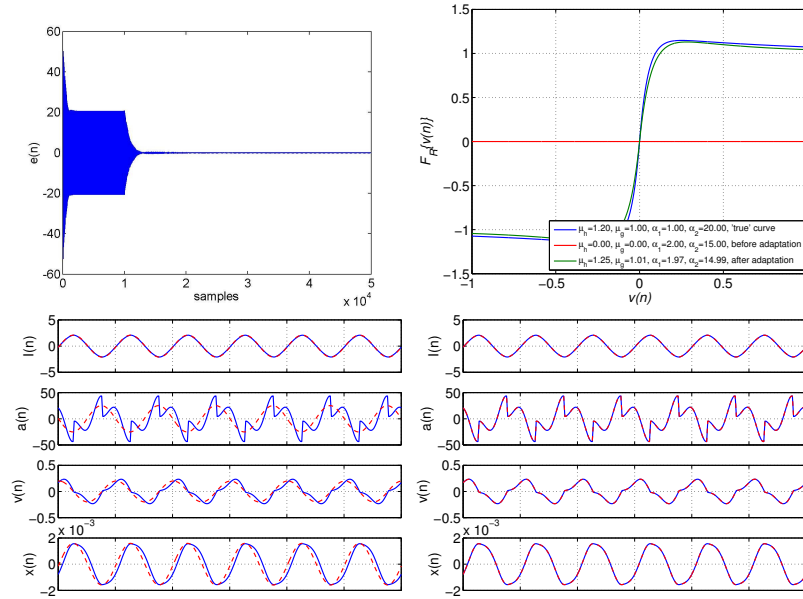


Figure 6: Simulation results, adaptation of friction curve, all other parameters exactly initialized, top: $e(n)$ (left) and friction curves (right), bottom: signals before (left) and after (right) adaptation.

e.g. $\mu_h > \mu_g$ and $\alpha_1 < \alpha_2$. The parameters before and after adaptation as well as the parameters of the 'true' system are given in the graphs. In Figure 6 all other parameters are assumed to be estimated exactly, whereas in Figure 7 B_l is chosen to be 10% to large. In the latter case the adaptation of the friction curve is bad compared to the first case, and in both cases α_1 and α_2 have not been changed very much from their initial values. But, in both cases the signals match very well after adaptation.

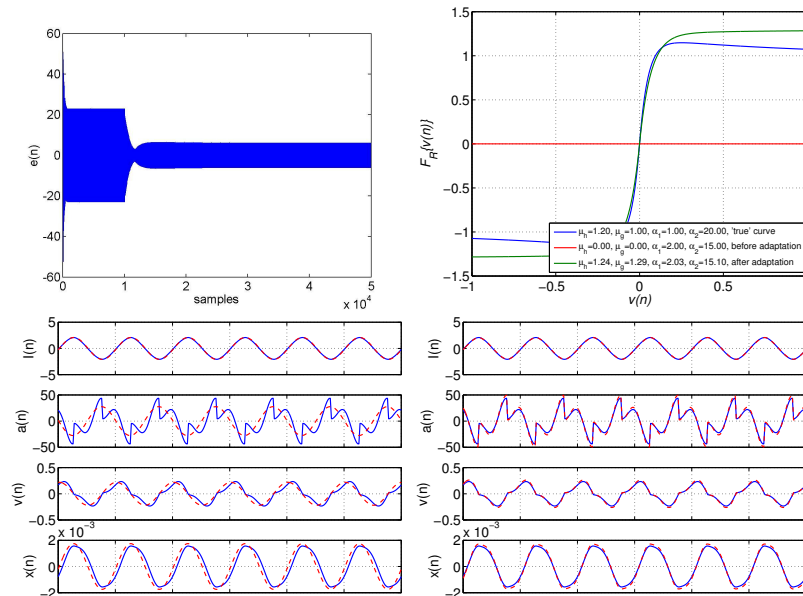


Figure 7: Simulation results, adaptation of friction curve, $B_l = 2.2 T_m$, all other parameters exactly initialized.

To successfully adapt the parameters it is important, that the parameters initially cho-

sen result in a stable model.

3 NEURAL NETWORK SECONDARY PATH MODEL

A common black-box model for nonlinear dynamic systems is the so-called time delay neural network (TDNN) [9]. I.e. a neural network like the one which is shown in Figure 8. It is constructed from the so-called multi layer perceptron (MLP), which consists of an input layer, an arbitrary number of hidden layers and an output layer. The hidden layers and the output layer consist of an arbitrary number of neurons, which are linear combiners followed by an activation function

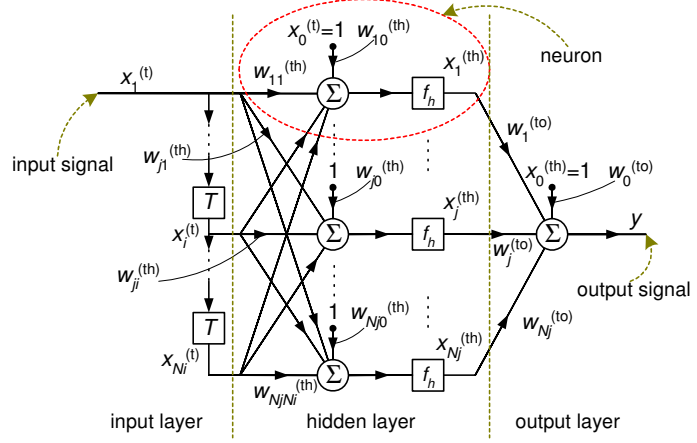


Figure 8: Time delay neural network

each. The latter is the nonlinear element in the neural network. The neurons have an additional input with fixed input signal, the so-called *bias*. All neuron inputs have weights (i.e. filter coefficients) which have to be adapted to fulfill the intended purpose of the network. When the input layer consists of a number of delayed values of a time signal, the neural network is called a time delay neural network.

The TDNN considered here is a pure feedforward network, i.e. without any internal feedback, with one hidden layer and a single neuron in the output layer. Thus, it can be seen as a nonlinear extension of the well-known FIR filter. The input-output equation of the TDNN given in Figure 8 can easily be read, i.e.

$$y(k) = w_0^{(to)} + \sum_{j=1}^{N_j} w_j^{(to)} f_h \left(w_{j0}^{(th)} + \sum_{i=1}^{N_i} w_{ji}^{(th)} x_i^{(t)}(k - i + 1) \right). \quad (31)$$

wherein $x_i^{(t)}(k - i + 1) = x_i^{(t)}$. In signal processing applications the activation function usually is chosen to be $f_h(x) = \tanh(x)$ which provides for positive and negative values. The output layer of a TDNN is usually chosen to have no activation function at all to allow arbitrary amplitudes at the output.

In [10] methods are given to estimate TDNN based models for nonlinear dynamic systems. The TDNN in Figure 8 is then called a NNFIR model (cf. Figure 9). When the output of the TDNN is fed back to the input of the TDNN, it is called a NNOE (neural network output error) model. This is the nonlinear counterpart to an IIR filter. In a similar manner NNARX and NNARMAX, etc. can be defined [10] which have their linear counterparts ARX and ARMAX, which are widely used in linear system identification [8].

The simplest algorithm to adapt the weights of the TDNN is the well-known back-propagation algorithm [9, 10]. A more sophisticated algorithm with much faster convergence speed and lower adaptation error is the Levenberg-Marquardt algorithm [10]. The

difficulty of nonlinear system identification is not due to the algorithm⁴ but due to other topics, i.e. finding a suitable set of test signals containing all frequencies and amplitudes, finding a suitable model structure like NNFIR, NNOE, etc. and finding the right size of the model, i.e. the number of input taps for the delayed input and output signals and the number of neurons. All together is not such a trivial task as it is usually in active noise control when estimating a linear FIR filter with the LMS algorithm and some white noise excitation.

Neural network based system identification tests were performed for the mechanical part of the sound source first, i.e. without the tube and using an accelerometer as error sensor. A random walk signal was used as test input to the shaker and input and output signals were recorded. These signals were used to train the network. Different signals including sinusoidal signals were used to verify the estimated models. The verification showed that the NNARX model resulted in much better models with smaller networks than the NNFIR model. It is assumed that the feedback inside the model structure shown in Figure 2, i.e. the nonlinear friction curve, is the reason for the need for output feedback. In other words, the NNARX structure fits better to the analytical structure, which was found with physical insight. The NNARX model uses the measured output signal along with the measured input signal in the training period. After training the model was verified as an NNOE model, because its output shall not be measured but simulated by the model itself. The same applies if the model will be used in active noise control applications. The best NNARX respectively NNOE model found used 2 output samples and 10 input samples and consisted of 19 neurons in the hidden layer [12].

When trying to estimate an extended neural network model, which includes the acoustic characteristics too, another problem appears. Due to the fact that an electro pneumatic sound source generates rather high amplitudes of random noise in addition to the desired tones test signals consisting of random noise with eventually varying amplitudes is not a very good choice. It might be helpful to use test signals with multiple sinusoids as is suggested in [13].

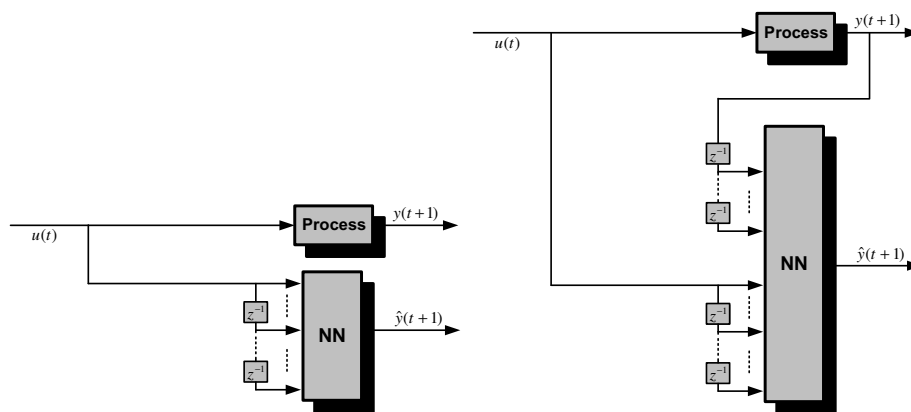


Figure 9: Nonlinear model structures using TDNN: NNFIR (left), NNARX (right) [10]

⁴In fact there exists a MATLAB-Toolbox for this purpose [11].

4 CONCLUDING REMARKS

Nonlinear modelling is needed when nonlinear sources shall be used in active noise and vibration control applications. Whereas modelling of secondary paths containing linear secondary sources is straightforward, this is not the case with nonlinear secondary paths. Even if ready-made black box models like time delay neural networks are used the choice of model structure, model size and type of test signals results in a lot of trial and error in order to yield an adequate model for control. Physical understanding of the source and its nonlinear behavior can help to choose the adequate model structure.

For the NNFIR model an algorithm for a feedforward active noise control scheme is given in [1] using a neural network based controller. It could be shown [3], that for control of harmonic sound, i.e. the purpose the electro pneumatic sound source is intended for, a simpler FIR filter controller [2] can also be used. This greatly reduces the computational burden necessary for the execution and adaptation of a neural network controller. Nevertheless, an algorithm for the NNOE secondary path model must still be derived, and this will be done by the authors in the near future. Also an algorithm will be derived, which includes the analytical time-discrete secondary path model shown in this paper into the feedforward control scheme.

ACKNOWLEDGEMENTS

This work is sponsored by the Deutsche Forschungsgemeinschaft – DFG (German Research Foundation), Project-No. Mo 390/10-2.

REFERENCES

- [1] C.H. Hansen, S.D. Snyder. *Active Control of Noise and Vibration*. (Chapman and Hall 1997).
- [2] A. Jakob, M. Möser. Nonlinear active noise control of harmonic sound by means of neural networks, *12th International Congress on Sound and Vibration - ICSV12*, 2005.
- [3] A. Jakob, M. Möser. Simulatorischer Vergleich von FIR-Filtern und neuronalen Netzwerken zum Einsatz als Feedforward-Controller in ANC-Anwendungen mit nichtlinearer Sekundärstrecke bei harmonischen Signalen, *Fortschritte der Akustik - DAGA 2006*, (annual conference of the german acoustic society - DEGA, published in german).
- [4] C.J. Chapman, A.G. Glendinning, A theoretical analysis of a compressed air loudspeaker, *Journal of Sound and Vibration*, 138(3):493–499, 1990.
- [5] A.G. Glendinning, P.A. Nelson, S.J. Elliott, Experiments on a compressed air loudspeaker, *Journal of Sound and Vibration*, 138(3):479–491, 1990.
- [6] L.A. Blondel, S.J. Elliott, Electropneumatic transducers as secondary actuators for active noise control, *Journal of Sound and Vibration*, 219(3):405–481, 1999.
- [7] F.X.Y. Gao, W.M. Snelgrove, Adaptive linearization of a loudspeaker, *ICASSP 91*, vol. 5, 3589–3592, 1991.
- [8] L. Ljung. *System Identification – Theory for the User*, 2nd ed., (Prentice Hall PTR, 1999).
- [9] S. Haykin. *Neural Networks, A Comprehensive Foundation*. 2nd ed. (Prentice-Hall Inc. 1999).
- [10] M. Nørgaard, O. Ravn, N.K. Poulsen, L.K. Hansen. *Neural Networks for Modelling and Control of Dynamic Systems*. (Springer-Verlag London Limited 2000).
- [11] M. Nørgaard. *Neural Network Based System Identification Toolbox*. Department of Automation, Technical University of Denmark, 2nd ed., 2000.
- [12] M. Wolff. Systemidentifikation von nichtlinearen Sekundärstrecken in active noise control Systemen mit Hilfe Neuronaler Netzwerke, masters thesis, Technical University of Berlin, 2006 (in german).
- [13] W. Svensson, U. Holmberg, Identification of an electro pneumatic loudspeaker using Hammerstein models, *ACTIVE 2002*.